



Assessment of slope instability with effects of critical displacement by using InSAR and FEM

Zeynep Sertabipoğlu¹ · Ümit Özer¹ · Hakan Tunçdemir²

Received: 18 July 2019 / Accepted: 22 January 2020 / Published online: 8 February 2020
© Saudi Society for Geosciences 2020

Abstract

A good knowledge of the mechanism of slope failure in open-cast mines can be understood by evaluating the intrinsic and extrinsic factors and their interactions in causing slope instability, and by gathering displacement information from periodical monitoring. Surface deformations, caused by mining activities at mine sites, are conventionally measured by using survey instruments such as levels, theodolites, total stations, GPS receivers, and photogrammetric cameras. However, conventional long-term monitoring techniques are insufficient due to unfavorable factors such as topographic structure and flora of the observation, urbanization rate, and time delays in obtaining results. Due to this fact that the Interferometric Synthetic Aperture Radar (InSAR) technique has become prominent in recent years as a method that uses satellite data to enable the detection of surface deformations and movements especially in very large areas. In this study, the mechanism of slope failure accurately detected by way of associating mechanical and physical information of the slopes with time-dependent deformation behavior (time series analysis) by periodically monitoring of displacements at the benches of a lignite open pit that experienced interruptions of production due to slope failures. Mining area has been periodically monitored by InSAR and data consisting of the time-dependent behavior of the deformations were correlated with the mechanical and physical property data that were obtained from back analysis of slope failure using finite elements method (FEM) approximation. In this context, a dynamic method was proposed that can predict the failure risk of the slopes at the site before the critical displacement values are not reached.

Keywords InSAR · FEM · Back analysis · Slope failure · Critical displacement

Introduction

Mining activities in open pits or underground mines will cause volume changes in the rock mass around a mine excavation as well as stress-induced deformative changes. Instability around the mine excavation emerges when the stress generated from mining activities exceeds the rock strength (Osasan 2012). In a previous study, Kayesa (2006) emphasized the importance of designating reference points at unstable areas at and around open pits to detect deformations occurring at these areas as

well as the importance of performing periodic and automatic monitoring of these points. These two researchers also mandated that a slope monitoring program is indispensable for the management of slope stability at an unstable site located in a pit where underground or open-pit mining is performed. It is very important to monitor and investigate the slopes accurately to detect the possible danger signals of a slope failure, and to thereby protect the personnel and the equipment. Various geotechnical designs may be developed to increase the safety coefficient, and proper bench designs may be developed to decrease the danger of falling rock. However, even if the slopes have protective slopes in their designs, they may still be subject to unexpected failure and deformation due to unknown geological structures, abnormal weather conditions, and seismic activities (Girard 2001).

Many researchers have tried to understand and analyze the mechanisms of slope deformation and failure at mines by using different techniques (Pumjan 1998; Chen 1994; Kollı 2001; Feng 1997; Gadri et al. 2015.; Wang et al. 2010; Ahmadi et al. 2019). One of the techniques developed by

Responsible Editor: Zeynal Abiddin Erguler

✉ Ümit Özer
uozer@istanbul.edu.tr

¹ Department of Mining Engineering, Faculty of Engineering, Istanbul University-Cerrahpaşa, Avcılar, Istanbul, Turkey

² Department of Mining Engineering, Faculty of Mines, Istanbul Technical University, Ayazaga, Istanbul, Turkey

the researchers for the analysis of slope stability is the numerical modeling (Deschamps 1993; Behrens da França 1997; Seo 1998; Loehr 1998; Maclaughlin 1997; Hwang 2000; Başar 2006). In the study of Sun (1983), slope stability was modeled by the finite elements method (FEM) with respect to the presence of water in pores. They observed that the presence of water in pores did not affect the safety coefficient (FS). They emphasized the importance of evaluating all the forces caused by water pressure with the forces at the node points used in the method, and they suggested that the FEM is more effective than the Bishop model in this context. Furthermore, it was reported that the stress area obtained with FEM is modeled in a relatively better manner than the slice method. The purpose of the study by Wanstreet (2007) was to analyze the effect of soil nail on slope stability coefficient of safety (FS) using FEM and to investigate the failure mechanism of the slope. In their study, slopes were analyzed with the shear-strength reduction technique (SRF). When the finite element method and SRF were combined, they were more successful compared to conventional methods, especially in complex geometries. This conventional approach makes the problem iterative and subsequently increases the analysis time and effort. However, in the proposed method, an intelligent method is used to update the new SRF based on the old values (Seyed-Kolbadi et al. 2019). In Benko's (1997) study, numerical modeling techniques were applied on complex slope stability problems. They reported that performing slope stability analysis with numerical modeling generated far more successful results compared to conventional methods such as limit balance. In their study, Akçakal et al. (2010) studied a slope movement that occurred at a foundation excavation opened without support during a collective housing construction project made in Göktürk, Istanbul. Their study was performed using back analysis with the help of FEM, and the results of tests made at the site and in a laboratory were compared with the results of the back analysis. Based on the results of the study, it was seen that while the tests made at the site and in laboratory represented only a limited region of the whole area, the study of slope failure with back analysis method facilitated the obtaining of shear strength data for that particular region in a more precise manner and contributed effectively to the conduct of improvement/reinforcement projects reliably and economically at the slopes where failure occurred.

Rowbotham (1995) stated that although numerous models have been developed to date for analyzing slope stability, these models require detailed geotechnical measurements to be taken in prior at the site. However, they also stated that after Geographical Information System (GIS) and Digital Elevation Models (DEM) are used, it becomes possible to conduct slope stability analysis at a regional level. They also claimed that these models are relatively more efficient compared to the other methods regarding the analysis of slope stability. In the study of Kjelland (2004), numerical models

were generated with geotechnical data, and information from GIS and simulations were used to evaluate the factors that affect slope failures. In the GIS environment, the data obtained with geotechnical measurement instruments were integrated with the site geometry and geology. Numerical models were calibrated according to the observed failure characteristic by accounting for the geologic controls and processes, and they were then used to delineate the sensitivity of the slope stability according to material properties and changing water table level.

Blesius (2002) investigated whether remotely acquired data is sufficient to generate values for critical parameters required by slope stability models and whether satellite images can be used instead of aerial photographs. Based on the results, they showed that geometric parameters can be estimated with remotely acquired data and that satellite images can substitute aerial photographs. A new methodology was also developed for the evaluation of slope failures. This approach integrates satellite-based images with local variables to determine the slope stability parameters and to allow generation of stable slope failure maps. It was stated that the developed methodology yielded positive result at the application area. In the study conducted by Catania et al. (2005), slope failures and mass movements were monitored with the InSAR technique and geomorphologic analysis was performed. Singhroy and Molch (2004) mentioned in their study that InSAR techniques were used for observing slope failures in recent studies. Akbarimehr et al. (2013) attempted to determine displacements at Sarcheshmesh's old landslide area located at northeast of Iran—whose failure mechanism is not well known—by using Envisat InSAR data and GPS observations, and continuous deformation maps were generated by generating InSAR time series analyses. Based on the results of the study, it was determined that displacements were less than 2–3 mm/year, and the results of the hydrogeological analyses showed that the landslide area where the study was conducted was not active due to the lack of hydrologically triggering factors in the last 10 years. However, it was reported that the Envisat InSAR data was inadequate for determining the displacement at the landslide area, and that it would be possible to obtain more precise and accurate results with new SAR data having higher temporal and spatial resolution, such as TerraSAR-X, instead of EnviSat satellite data.

Hartwig et al. (2013) used PSI (Persistent scatterer Interferometry) to monitor an iron open-pit mine in Carajas, Brazil. Eighteen scenes using TerraSAR-X acquired during the dry season. While most of the study area was stable, high rates of strain were detected in dumps (312 mm/year). For the same mine, in Paradella et al. (2015) study, instabilities were monitored through an integrated SAR analysis based on a data-stack of 33 TerraSAR-X images. Raventós and Sánchez (2018) studied a full InSAR application on a large-scale open coal mine in a monitoring program.

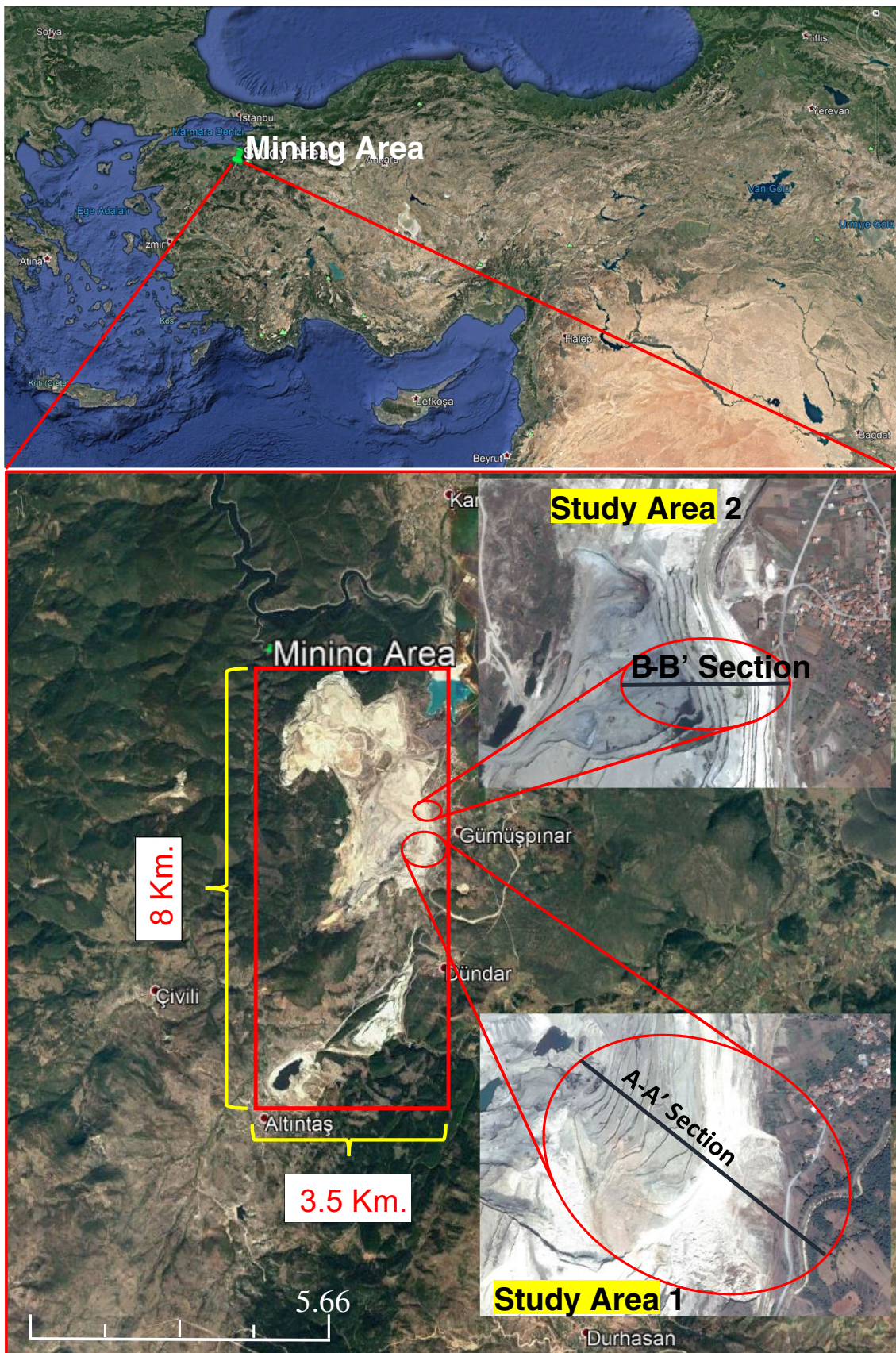


Fig. 1 Location map of study areas 1 and 2

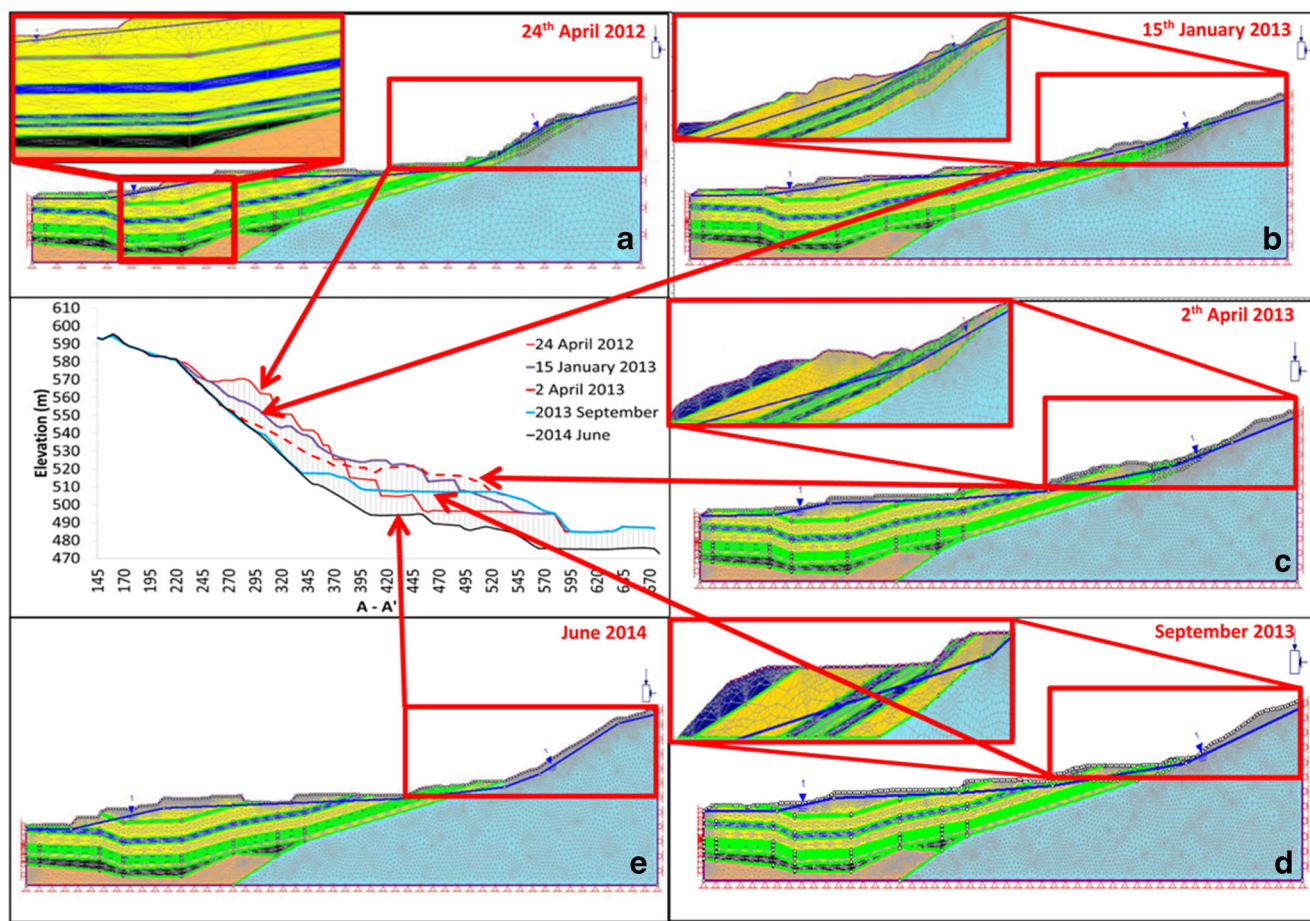


Fig. 2 Geometric model of a the first failure, b the second failure, c the third failure, d the first excavation, and e the second excavation

Slope failure at open-pit mines can be fully elucidated with the evaluation of internal and external factors and their interaction and with the displacement data obtained from periodic observations. For this reason, in order to ensure the continuity of production and the safety of the people and structures at sites where open-pit mining is conducted, it is necessary to monitor the displacements occurring on the surface of the ground and to observe whether these displacements reach

the critical risk value. In addition, it is necessary to consider the geological structure, rock mass characteristics, hydrogeological conditions, and the method of production.

The aim of this study is to develop an InSAR-based dynamic monitoring technique providing an early warning mechanism that may help preventing possible slope failures in a large-scale open-cast coal mine. In order to ensure this phenomenon, the slope movements, which were experienced

Table 1 Properties of materials

Parameters	Materials						
	Tuffite	Marl	Sandstone	Weak zone	Coal	Claystone	Limestone
Unit volume weight (kN/m ³)	19.00	16.41	18.46	17.65	12.46	20.0	27.37
Friction angle (ϕ) (°)	10.0	25.0	26.0	11.0	20.7	15.0	38.0
Cohesion (c) (kPa)	18.0	13.0	56.0	5.0	325.0	180.0	500.0
Compressive strength (kPa)	2200	9000	9800	2200	3800	11,000	45,100
Tensile strength (kPa)	220	900	980	220	380	1100	4510
Elastic modulus (kPa)	10,000	400,000	335,000	50,000	500,000	394,000	2,000,000
Poisson ratio	0.32	0.30	0.33	0.35	0.20	0.35	0.28
Stress ratio	Field stress: gravity, stress ratio: 0.5 (horiz/vert)						

Table 2 Shear strength parameters and SRF values of the failures and excavations

	Undisturbed		Disturbed				Undisturbed			
	24th of April 2012 1st failure		15th of January 2013 2nd failure		2nd of April 2013 3rd failure		September 2013 1st excavation		June 2014 2nd excavation	
	ϕ^*	c^{**}	ϕ	c	ϕ	c	ϕ	c	ϕ	c
Tuffite	10	18	10	18	10	18	10	18	10	18
Marl	25	13	18	13	18	13	18	13	18	13
Sandstone	26	56	26	56	26	56	26	56	26	56
			1st disturbed		2nd disturbed		3rd disturbed			
Disturbed Tuffite			7	14	4.71	9.35	4.24	8.42		
Disturbed Marl			20	10	13.72	6.71	12.40	6.04		
Disturbed Sandstone			21	46	14.44	30.87	13.06	27.81		
Weak zone	11	5	11	5	11	5	11	5	11	5
Coal	20.7	325	20.7	325	20.7	325	20.7	325	20.7	325
Claystone	15	180	15	180	15	180	15	180	15	180
Limestone	38	500	38	500	38	500	38	500	38	500
SRF***	0.64		0.69		0.73		0.93		1.14	

* ϕ : friction angle ($^{\circ}$) ** c : cohesion (c) (kPa) ***SRF: strength reduction factor

at a coal open-pit mine benches between 2012 and 2015, and which were resulted by production interruptions due to slope failures, were analyzed together by FEM and the InSAR with TerraSAR-X satellite images of the site within the Repeat Orbit Interferometry Package (ROI-PAC) program. Accordingly, time-dependent displacement graphics (time series analysis) were generated and slope stability analyses were performed with the help of back analysis.

Introduction of the mining area

The mining area is located in Bursa Province, Turkey. It is at a distance of 21 km from the Orhaneli District and 300 m from the village of Gümüşpınar. Its elevation is 500 m from sea level (Fig. 1).

Geology of the mining area

Geology of mine has a complex structure. Stratigraphic time scale of Pre Neogene structures consist of metamorphic schists, recrystallized limestone, and serpentinites. Neogene formation scales covers from clastic rocks in the lowest level. Clastic rocks contains conglomerates, sandstones, gravels, and clays at the bottom side and marl and tuffs consisting of lignite seams at the top side which are coal reserves of Orhaneli Open Pit Mine. Volcano sedimentary and volcanic rocks are settled on them (Tunçdemir et al. 2013; Sertabipoğlu 2016).

History of the study areas and back analysis

Study area 1

The study area 1 (Fig. 1), the east slopes of the Gümüşpınar sector, was chosen because three slope failures were experienced on 24th of April 2012, and 15th of January and 2nd of April 2013. In order to detect the slope failure mechanism and excavations, 2D finite element analysis was performed by using Phase2 v. 8.0 software for back analysis. A pre-failure geometric model was created along A-A' section (Fig. 1 and Fig. 2) at first. Mechanical properties of seven material (Table 1) and an underground water table were then defined in the model (Fig. 2a). The shear strength values in failure zone at the time of the second and third failures were taken as the first and second disturbed material strength values, respectively (Table 2), and assigned to the materials in failure zone of geometric model (Fig. 2b and c).

After the third failure (2nd of April 2013), there was still some slope instability hazard despite the naturally decreasing slope angle after each failure. A part of the sliding mass was excavated and removed by the enterprise in September 2013 to relax weight and to prevent sliding the fallout mass more into the production area where the production activity would be carried out in the lower codes of the failure zone. Shear strength values for the third failure (2nd of April 2013) were used in geometric modeling (Fig. 2d) as the third disturbed material strength values (Table 2). However, despite those removal activities, the slope stability could not be completely fixed.

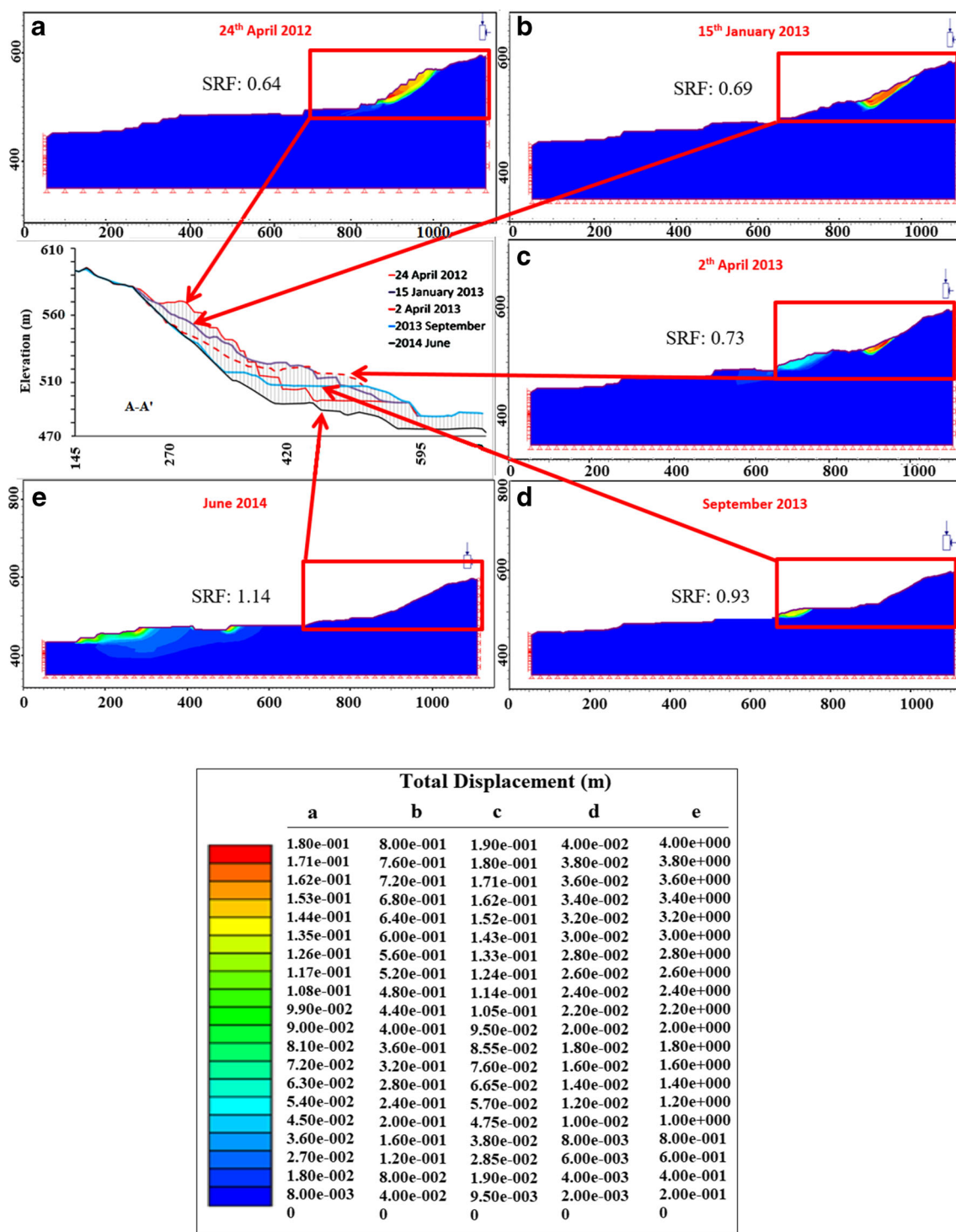


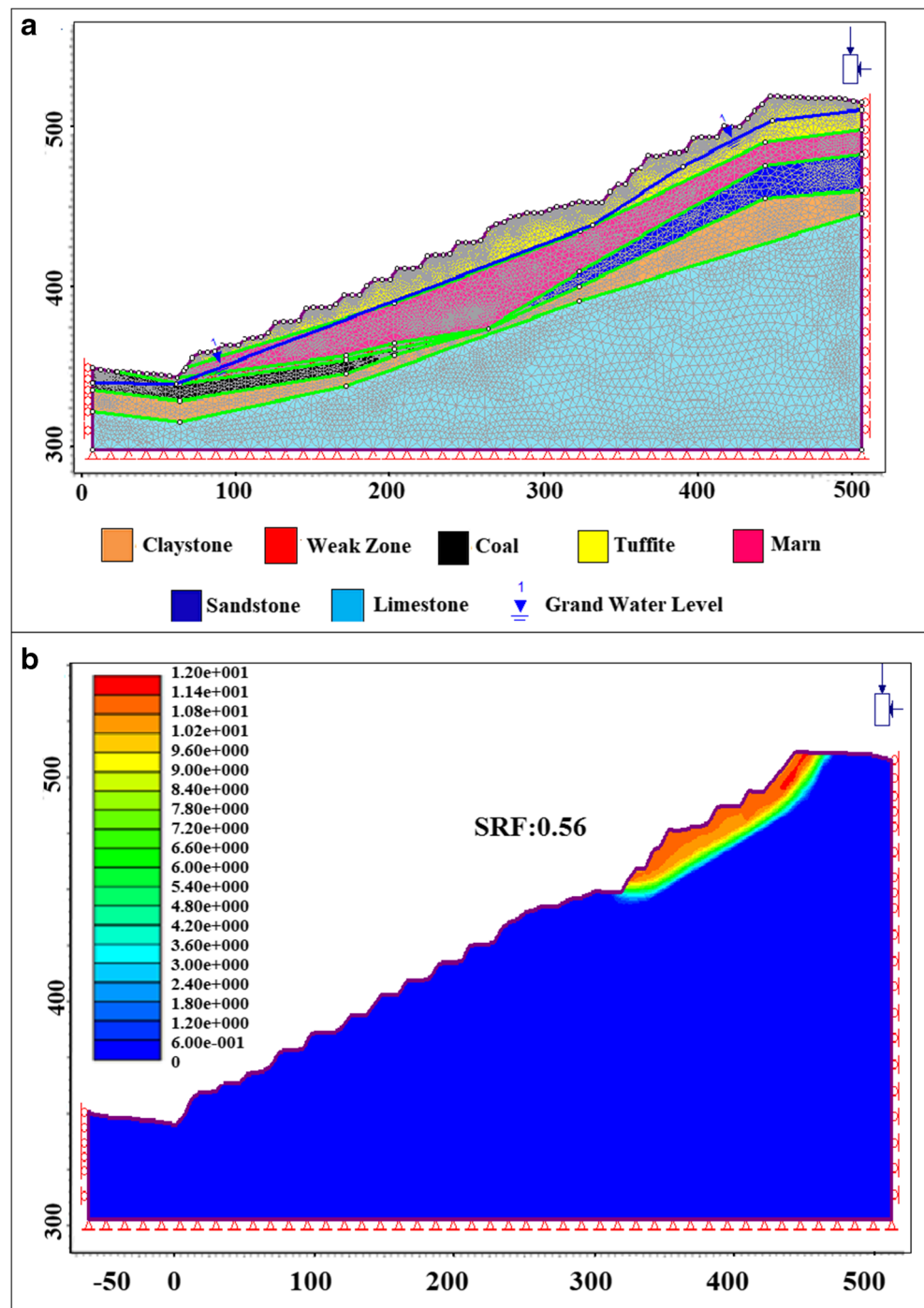
Fig. 3 Analysis result and SRF value of a the first failure, b the second failure, c the third failure, d the first excavation, and e the second excavation

Therefore, all sliding mass was excavated down to bed-rock level (limestone) and removed from slope, in June 2014. Seven materials and underground water table have been defined to the geometric model showing the latest situation (Fig. 2e). Material properties seen in

Table 1 were assigned to the model since all disturbed materials have been removed completely by the excavation.

The failure analysis results of the slope (SRF values) are shown in Table 2 and Fig. 3a–e. It is predicted that the

Fig. 4 a Geometric model and b analysis result of failure occurred in the study area 2



instability of benches would remain consequently while the excavation is going on for coal production.

Study area 2

A new failure occurred on 19 January 2015, at a different location to the north of the slope area after failures experienced 2012 and 2014 (Fig. 1). 2D finite element analysis were

performed by Phase2 v. 8.0 software for back analysis. In the analysis of this failure, a pre-failure cross section (B-B' section) was generated by utilizing the production map of December 2014 (Fig. 1), which shows and represents the geometric structure before the failure occurred. Material properties (Table 1) were analyzed from the undisturbed materials (Fig. 4). As a result of the slope stability analysis, SRF value was found to be 0.56 (Fig. 5). It can be seen from the Fig. 5

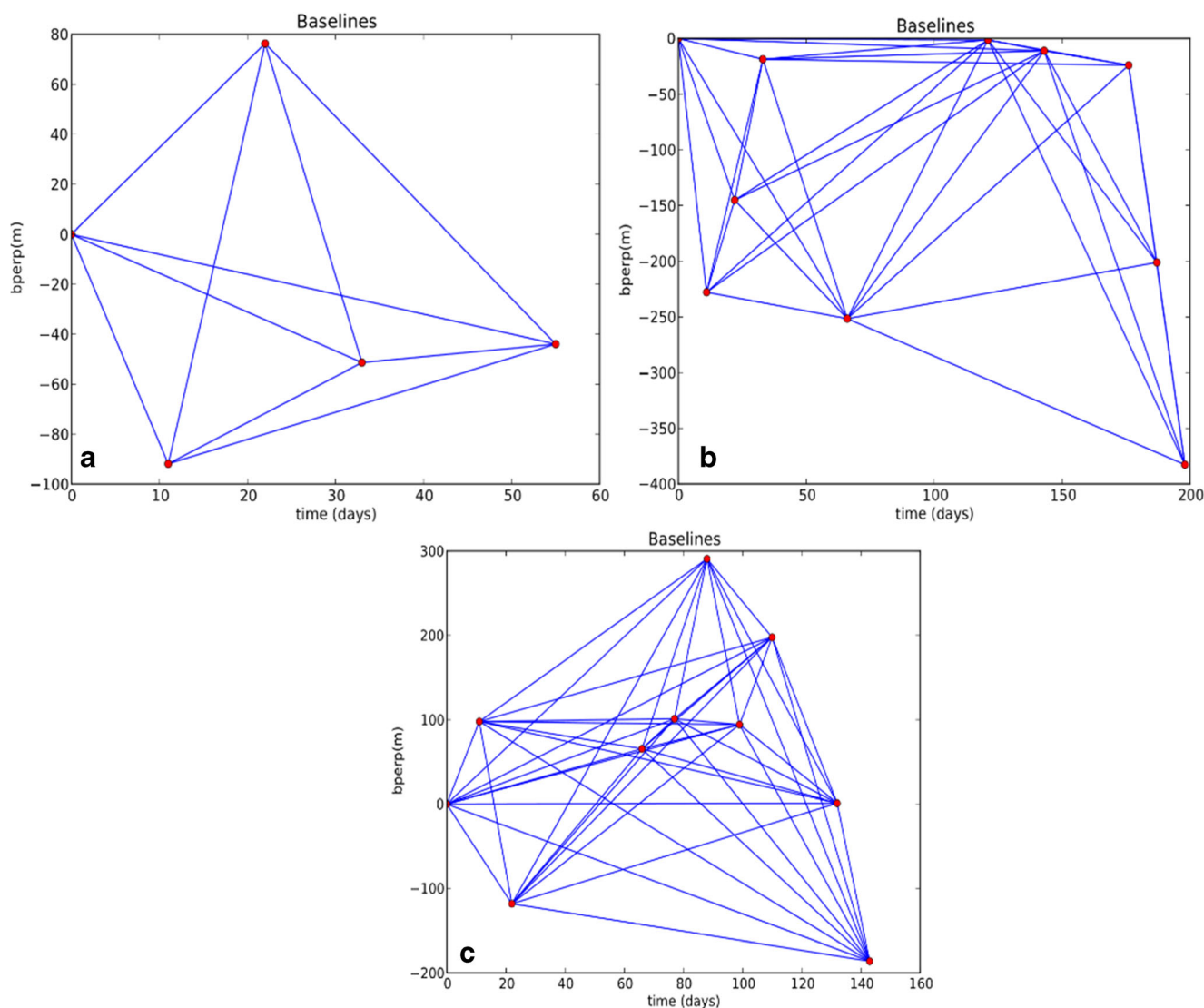


Fig. 5 Baseline graph of TerraSAR-X satellite images of the year 2012 (a), 2013 (b), and 2014 (c) (vertical axis; perpendicular component of the distance (baseline) between the satellite positions in two images, time (days); temporal difference between two images)

that there is a possibility of new failures at the lower benches of the slope towards the inside of the pit, unless precautions are taken after the failure occurred in January.

Analysis of InSAR data

Radar images derived from the TerraSAR-X (TSX) satellite of the German Aerospace Center (DLR) were used. In this study, 26 satellite images between 2012 and 2015 were obtained in HH (horizontal-horizontal) polarization, Strip Map (high-resolution) mode, and descending direction (Table 3).

Due to the lack of satellite images of the site to be analyzed for certain months of the years 2012, 2013, and 2014 in the obtained satellite images, the existing images were divided into 3 groups, namely, groups of 2012, 2013,

and 2014–2015 (Table 4). TerraSAR-X satellite images were analyzed with Linux-based open-source Repeat Orbit Interferometry PACKAGE (ROI-PAC) program, and 3 arc-second ASTER Digital Elevation Model (DEM) with 10-m sensitivity was used to eliminate the topographic effect in the study.

Baseline geometry was studied for all three groups separately (Fig. 5a–c). As seen in the figures, due to the fact that a large spatial (bperp) and temporal difference between some satellite images will decrease the interferogram coherence (decreasing of the accuracy of displacement values), 11 interferograms were selected for analysis purposes out of 33 for the year 2013, and 10 interferograms were selected for analysis purposes out of 33 for the years 2014–2015. All interferograms (10 interferograms) for the group of year 2012 were used for analysis.

Table 3 TerraSAR-X data set

No.	IM	P	Date	D or A
1	Strip map	HH	16.01.2012	D
2	Strip map	HH	27.01.2012	D
3	Strip map	HH	07.02.2012	D
4	Strip map	HH	18.02.2012	D
5	Strip map	HH	11.03.2012	D
6	Strip map	HH	24.01.2013	D
7	Strip map	HH	04.02.2013	D
8	Strip map	HH	15.02.2013	D
9	Strip map	HH	26.02.2013	D
10	Strip map	HH	31.03.2013	D
11	Strip map	HH	25.05.2013	D
12	Strip map	HH	05.06.2013	D
13	Strip map	HH	16.06.2013	D
14	Strip map	HH	19.07.2013	D
15	Strip map	HH	30.07.2013	D
16	Strip map	HH	10.08.2013	D
17	Strip map	HH	10.09.2014	D
18	Strip map	HH	21.09.2014	D
19	Strip map	HH	02.10.2014	D
20	Strip map	HH	15.11.2014	D
21	Strip map	HH	26.11.2014	D
22	Strip map	HH	07.12.2014	D
23	Strip map	HH	18.12.2014	D
24	Strip map	HH	29.12.2014	D
25	Strip map	HH	20.01.2015	D
26	Strip map	HH	31.01.2015	D

IM image mode, P polarization, HH horizontal-horizontal, D descending, A ascending

Interferograms generated for year 2012, 2013, and 2014 together with the study area are shown in Fig. 6. The unwrapped form of interferograms generated for year 2012 (120127–120311) is shown in Fig. 6(a). The unwrapped form of the interferogram obtained from selected satellite images (coherence higher than 0.6) between the dates of 130719–130730 belonging to 2013 is shown in Fig. 6(b). The unwrapped form of the interferogram obtained from selected satellite images between the dates of 141115–141126, belonging to 2014–2015, is shown in Fig. 6(c).

The interferometric phase is always noisy due to the effect of water vapor and temporal-spatial changes in the atmosphere. In order to reduce the amount of noise in the interferogram and increase coherence, the step after the creation of the interferograms is the filtering step. Sun et al. (2013) reduced the amount of noise by 79.5% and found 9 to 32% better results than the weighted power spectrum filter by

Table 4 TerraSAR-X data set (in black) and dates of slope failures and excavations (in red)

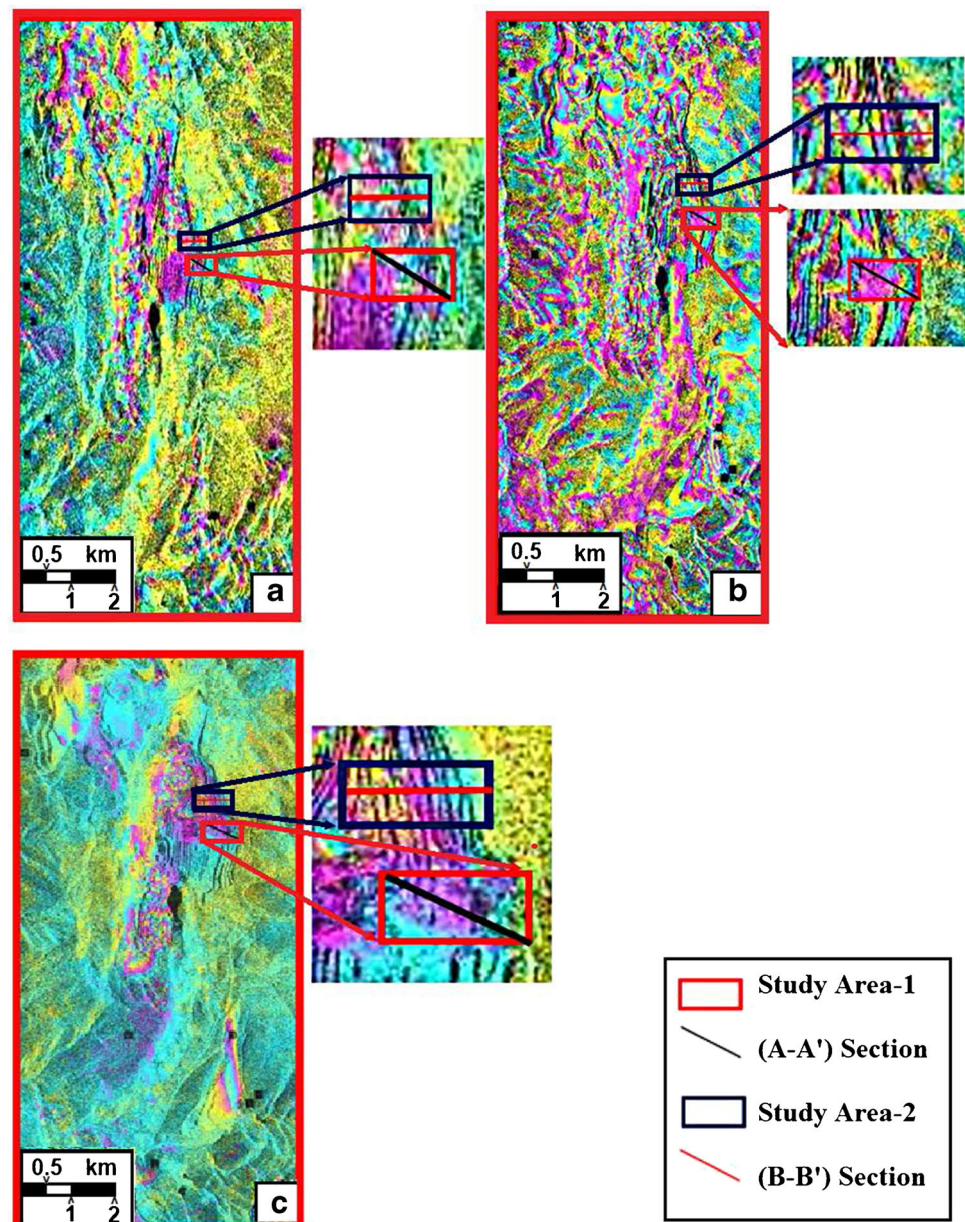
Years	TerraSAR-X data set	Date of failures and excavations
2012	16.01.2012	
	27.01.2012	
	07.02.2012	
	18.03.2012	
	11.03.2012	
2013		24 April.2012
		15 January 2013
	24.01.2013	
	04.02.2013	
	15.02.2013	
	26.02.2013	
	31.03.2013	
		02 April.2013
	25.05.2013	
	05.06.2013	
2014	16.06.2013	
	19.07.2013	
	30.07.2013	
	10.08.2013	
		September 2013
		June 2014
	10.09.2014	
	21.09.2014	
	02.10.2014	
	15.11.2014	
2015	26.11.2014	
	07.12.2014	
	18.12.2014	
	29.12.2014	
		19.January 2015
2015	20.01.2015	
	31.01.2015	

modifying the weighted power spectrum filter (Goldstein and Werner 1989). In this study, the modified weighted power spectrum filter was used.

Generation of time-displacement (time series) graphics

Five points were selected along the cross-section route used for slope stability analysis (Fig. 7(a)), and a single time series was generated by averaging the displacements at each point belonging to the period between the years 2012–2013 (Fig. 7(b)). As seen in Fig. 7(a), it was also determined how much the points determined for time series displaced during the

Fig. 6 Unwrapped interferogram of **a** 120127–120311, **b** 130719–130730, and **c** 141115–141126



failure with a program that generated analysis via FEM. In Fig. 7(b), a displacement up to 3 cm can be seen in the failure on 24 April 2012 (1st failure), the 2nd failure occurred 250 days after the first failure, and the 3rd failure occurred after the 2nd failure with an additional displacement of 3 cm, with the displacement persisting after the failure (up to 6 cm). Behavior of the movement before the failure is also seen in Fig. 7.

Five points were selected along the cross-section route used for slope stability analysis for years 2012–2013 to determine the displacements for year 2015

(Fig. 8(a)) and a single time series was generated averaging displacements at these points (Fig. 8(b)). As seen in Fig. 8(a), the displacement of the points for the time series was also determined using a program that performs analyses via FEM during the failure. As seen in Fig. 8(b), the displacements and the behavior of the movement before the failure of 19 January 2015 are also shown. Sufficient information could not be obtained about the movement after the failure due to the fact that the number of images after the failure was not sufficient.

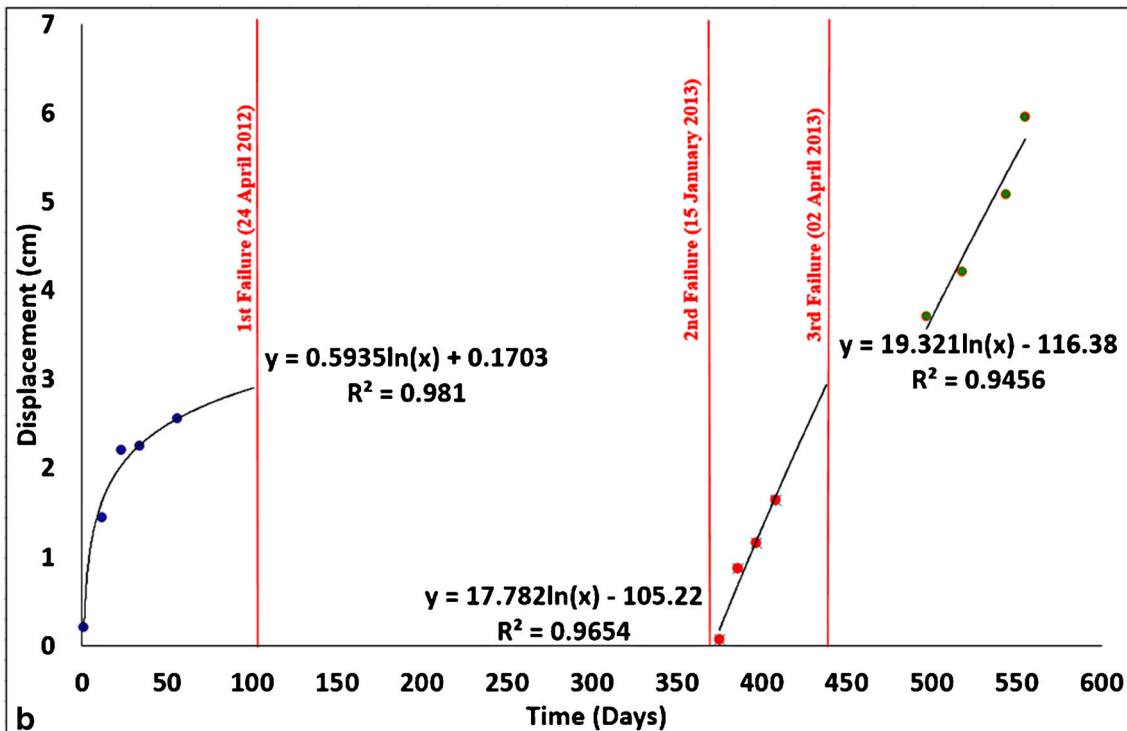
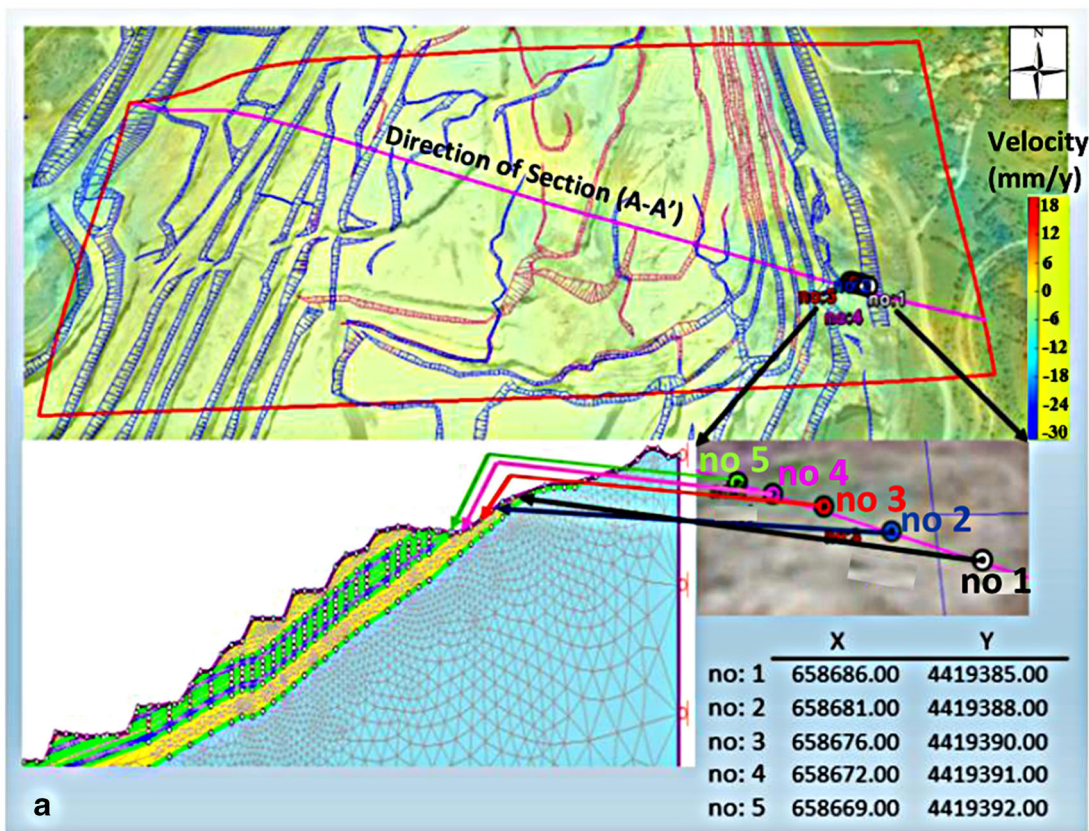
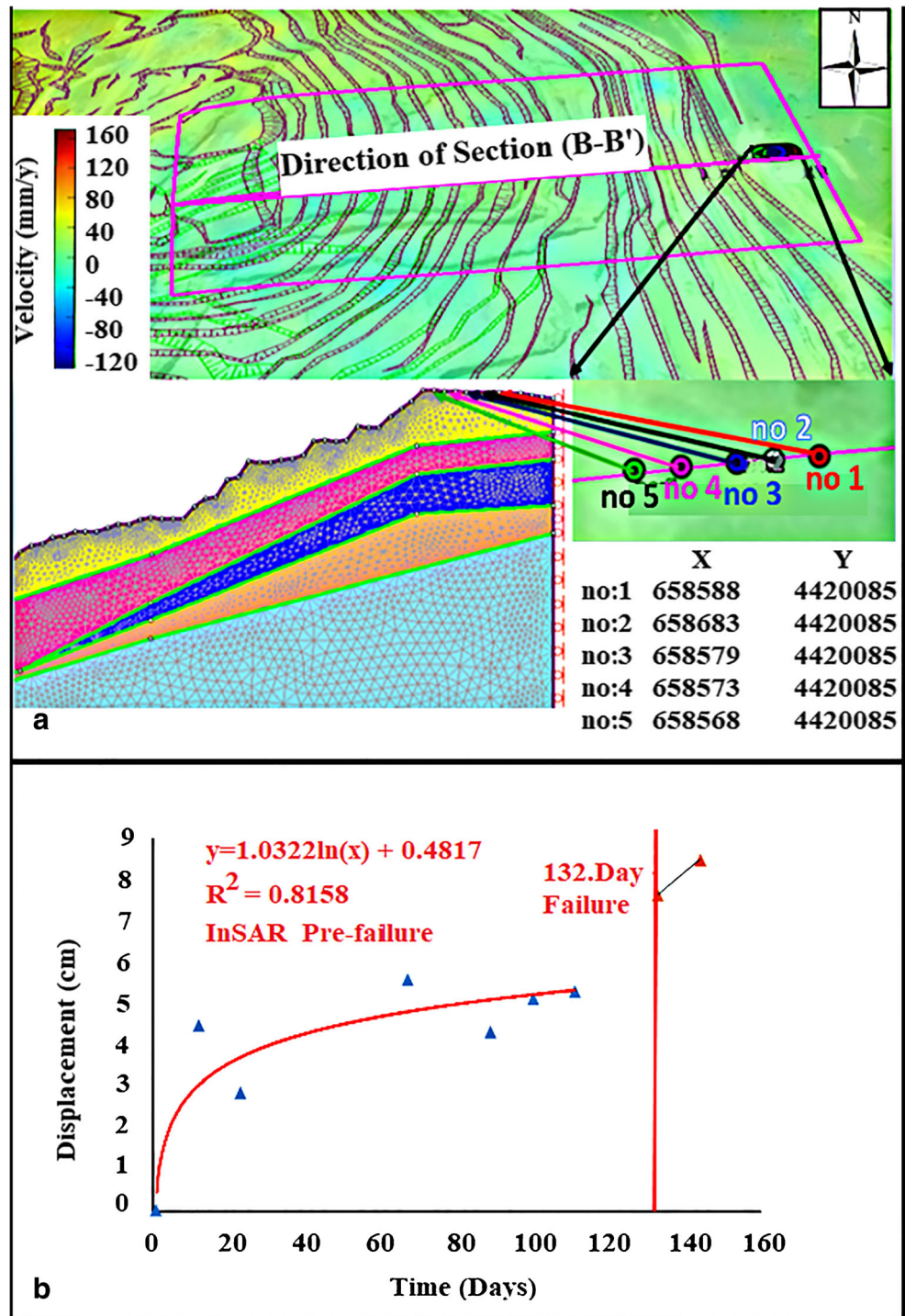


Fig. 7 The location of the points of the displacement values (a) and displacement-time graph (b) between 2012 and 2013

Fig. 8 The location of the points of the displacement values (a) displacement-time graph (b) for 2015



Evaluation of InSAR and finite elements analysis results simultaneously

The time, the amount of displacement, and the safety coefficients obtained from two- and three-dimensional finite element analyses and InSAR results were used to examine the relationship of these parameters all together. Acceptable

strong level relationships were identified among them, and charts that will enable the determination and estimation of the critical displacement amount that may cause slope failure, were developed. These nomogram charts are presented in Figs. 9, 10, and 11. When these charts are examined, it can be seen that the displacement values obtained from the analysis conducted via FEM and those obtained from the analysis

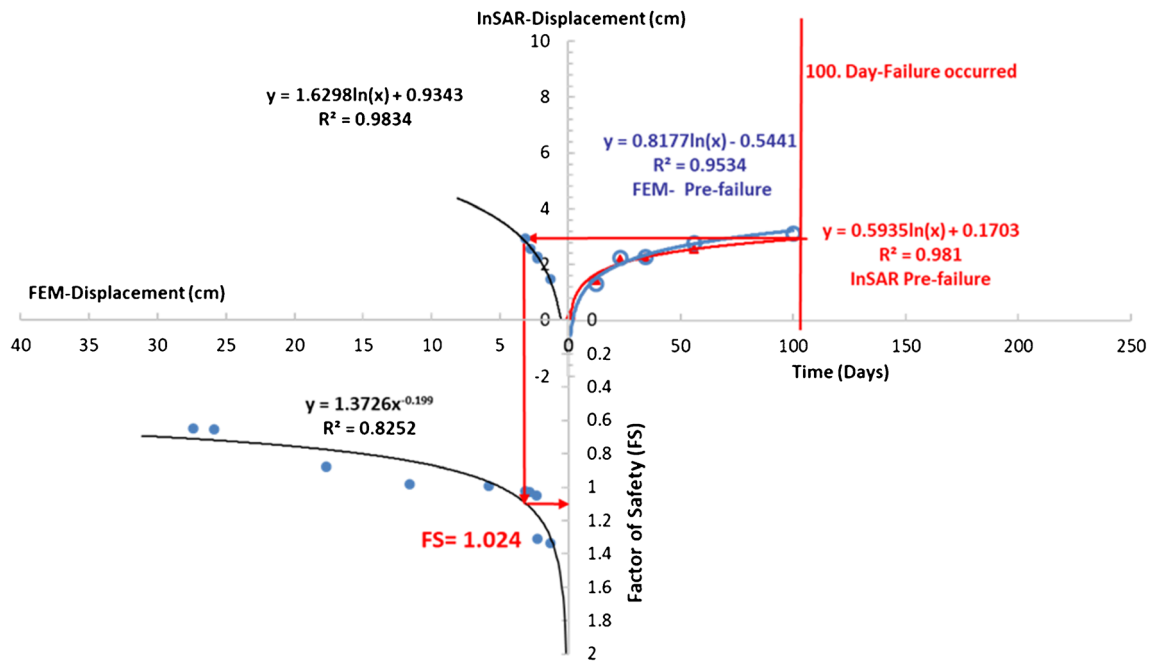


Fig. 9 Developed nomogram for failure occurred in 2012

made with InSAR are very close to each other, exhibiting a similar tendency. For this reason, it can be easily estimated which amount of displacement will be at the critical safety coefficient, or what the critical safety coefficient will be at critical displacement amount.

As seen in Figs. 9, 10, and 11, it is possible to monitor the displacement amount at which the safety coefficient is at

balance (SRF: 1.24, 0.99, or 0.97) and to take the necessary precautions. These charts also point out these slopes in balance will begin to fail after what period/amount of time. It can also be seen from these charts that the failure dynamic of each slope changes from year to year, depending on internal and external factors, such as its geometry and mechanical properties. Slope failures can be prevented by periodically monitoring the

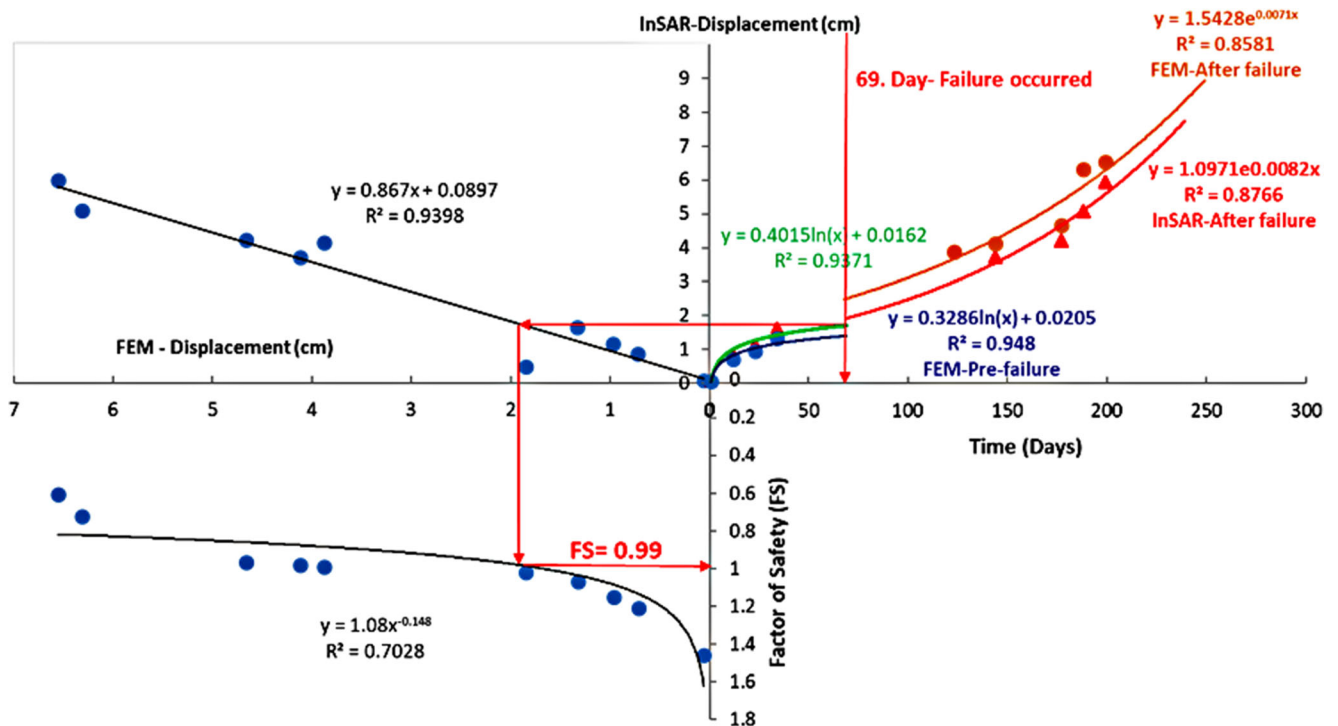


Fig. 10 Developed nomogram for failure occurred in 2013

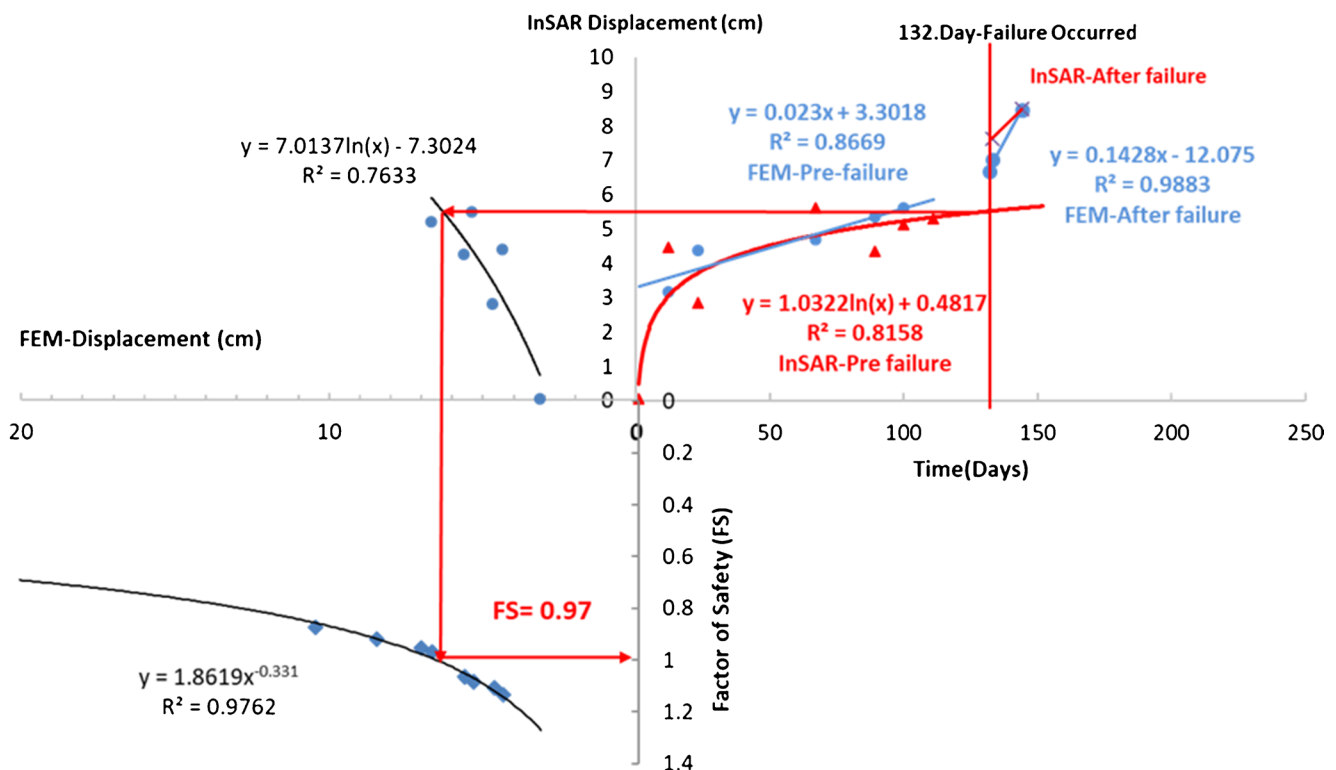


Fig. 11 Developed nomogram for failure occurred in 2015

displacements, and frequently determining the mechanical properties of the slope.

Conclusions

In this study, charts developed on a yearly basis were used to establish the relation between the mechanical properties of the study area and the periodically obtained displacement amounts, and it was shown in these charts that the failure dynamic of the slope changes from year to year, depending on internal and external factors, such as its geometry and mechanical properties and the status of the underground water.

Through the analysis of the satellite images of the site between the years 2012 and 2015 by using the InSAR method, we concluded that it will be possible to determine the dynamics of the movements at the site's slopes before the failure occurs, and that it will be possible to foresee the failure risk of the slopes at the site before the critical displacement values are reached.

In the future studies related to this subject, the safety factors of the slopes in the mine sites can be updated by taking into account the current geometrical, physical, and mechanical properties and the displacement values monitored of the slope. We concluded that the charts proposed for this study can be dynamically updated by different rock conditions encountered in the media throughout the continuous excavation.

Acknowledgments The authors sincerely thank Dr. Orhan Akyılmaz, Dr. Özgün Akçay, Dr. Mahdi Motagh, and Dr. Shimon Wdowinski and his scientific team for obtaining TerraSAR-X data and helping process of SAR images. This study was supported by Scientific Research Project Coordination Unit of Istanbul University-Cerrahpasa, Project number: 43316, Technical University of Istanbul - BAP Project number: 34256, and the Scientific and Technological Research Council of Turkey (TUBITAK), "2214-A International Research Scholarship during Ph.D. studies.

References

- Ahmadi R, El Mayl M, Dlalal M (2019) Ultimate slope design in open pit phosphate mine using geological and geomechanical analysis: case study of Jebel Jebbeus. Arab J Geosci 12:280–214. <https://doi.org/10.1007/s12517-019-4333-0>
- Akbarimehr M, Motagh M, Haghshenas-Haghighi M (2013) Slope stability assessment of the Sarcheshmeh landslide, Northeast Iran, investigated using InSAR and GPS observations. Remote Sens 5(8): 3681–3700. <https://doi.org/10.3390/rs5083681>
- Akçakal Ö, Aykut Ş, Öztoprak S, Durgunoğlu T (2010) Şev stabilitesi analizinde geri hesap yöntemi kullanılarak bir vaka analizi: Göktürk kayması, Zemin mekaniği ve temel mühendisliği 13. Ulusal Kongresi, İstanbul, pp 441–452 (In Turkish)
- Başar E (2006) Modelling of landslide triggering mechanisms, Boğaziçi University, İstanbul, Msc., p.164
- Behrens da França P R (1997) Analysis of slope stability using limit equilibrium and numerical methods with case examples from the Aguas Claras mine, Master's thesis, Queen's University, Brazil
- Benko B (1997) Numerical modelling of complex slope deformations, thesis (PhD). University of Saskatchewan, Saskatoon, p 278

- Blesius LJ (2002) A satellite based methodology for landslide susceptibility mapping incorporating geotechnical slope stability parameters, thesis (PhD), University of Iowa, USA, p.248
- Catania F, Farinaa P, Morettia S, Nicob G, Strozzi T (2005) On the application of SAR interferometry to geomorphological studies. Estimation of landform attributes and mass movements. *Geomorphology* 66:119–131
- Chen G (1994) A study on the application of probabilistic methods to slope stability problems, thesis (PhD), University of Toronto, Toronto
- Deschamps RJ (1993) A study of slope stability analysis, thesis (PhD). Perdue University, USA
- Feng P (1997) Probabilistic treatment of the sliding wedge, Master's Thesis, University of Manitoba, p.102
- Gadri L, Hadji R, Zahri F, Benghazi Z, Boumezbeur A, Laid BM, Rais K (2015) The quarries edges stability in opencast mines: a case study of the Jebel Onk phosphate mine. NE Algeria. *Arab J Geosci* 8: 8987–8997. <https://doi.org/10.1007/s12517-015-1887-3>
- Girard JM (2001) Assessing and monitoring open pit mine high-walls, proceedings of the 32nd annual institute of mining health. Safety and Research, Roanoke, VA, pp 59–171
- Goldstein RM, Werner CL (1989) Radar interferogram filtering for geophysical applications. *Geophysical Research Letters* 25, 4035–4038.
- Hartwig M, Paradella W, Mura J (2013) Detection and monitoring of surface motions in active open pit iron mine in the amazon region, using persistent scatterer. Interferometry with terrasars-x satellite data. *Remote Sens* 5:4719–4734
- Hwang J A (2000) Experimental and numerical investigation of three-dimensional stability of slopes, University of Colorado, , PhD., p.218
- Kayesa G (2006) Prediction of slope failure at Letlhakane Mine with The Geomos Slope Monitoring System, International Symposium on Stability of Rock Slopes In Open Pit Mining And Civil Engineering Situations, s44, p. 606–607
- Kjelland N H (2004) Slope stability analysis of Downie Slide: numerical modelling and GIS data analysis for geotechnical decision support, Master's Thesis. Queen's University, p. 237
- Kolli SPB (2001) Analyses of coal extraction and spoil handling techniques in mountainous areas. West Virginia University, Master's Thesis
- Loehr J E (1998) Development of Ahybrid limit equilibrium-finite element procedure for three-dimensional slope stability analysis, thesis (PhD), University of Texas, p. 399
- Maclaughlin M M (1997) Discontinuous deformation of analysis of the kinematics of landslides, thesis (PhD), University of California, p. 117
- Osasan K S (2012) Open-Cast Mine Slope Deformation and Failure Mechanisms Interpreted From Slope Radar Monitoring”, University of the Witwatersrand, Johannesburg, Phd.,p.222
- Paradella WR, Ferretti A, Mura JC, Colombo D, Gama FF, Tamburini A, Santos AR, Novali F, Galo M, Camargo PO, Silva AQ, Silva GG, Silva A, Gomes LL (2015) Mapping surface deformation in open pit iron mines of Carajás Province (Amazon region) using an integrated SAR analysis. *Eng Geol* 193:61–78
- Pumjan S (1998) A local probabilistic approach for slope stability analysis. Michigan Technological University, Thesis (PhD)
- Raventós, J, Sánchez C (2018) The use of InSAR for monitoring slope stability of rock masses, ISRM 1st international conference on advances in rock mechanics - TuniRock 2018, 29–31 march 2018, Hammamet, Tunisia
- Rowbotham D N (1995) Applying a GIS to the modelling of slope stability in Phewa Tal watershed, Nepal, Thesis (PhD), University of Waterloo
- Seo Y K (1998) Computational methods for elasto-plastic slope stability analysis with seepage, thesis (PhD), University of Iowa, p.166
- Sertabipoğlu Z (2016) Monitoring of open pit slope movements by using InSAR and slope stability analysis, Istanbul University, PhD thesis, p. 227
- Seyed-Kolbadi SM, Sadoghi-Yazdi J, Hariri-Ardebili MA (2019) An improved strength reduction-based slope stability analysis. *Geosciences* 9:55. <https://doi.org/10.3390/geosciences9010055>
- Singhroy V, Molch K (2004) Characterizing and monitoring rockslides from SAR techniques. *Adv Space Res* 33:290–295
- Sun F (1983) Finite element analysis of slope stability including pore pressure”, University of Wyoming, Laramie, Msc., p.94
- Sun Q, Li Z, Zhu J, Ding X, Hu J, Xu B (2013) Improved Goldstein filter for InSAR noise reduction based on local SNR. *J Cent S Univ Technol* 20:1896–1903
- Tunçdemir H, Güçlü E, Akçay Ö, Akyılmaz O, Yılmaztürk S, Motagh M (2013) A methodology for deformation control with InSAR: Orhaneli open pit mine case study, 23rd international mining congress and exhibition of Turkey. Turkey, Antalya, pp 211–217
- Wang Y, Cao Z, Au SK (2010) Efficient Monte Carlo simulation of parameter sensitivity in probabilistic slope stability analysis. *Comput Geotech* 37:1015–1022
- Wanstreet P (2007) Finite element analysis of slope stability, Master's Thesis, West Virginia University, p. 83